## ORIGINAL ARTICLE

# Disruption of mindin exacerbates cardiac hypertrophy and fibrosis

**Zhou-Yan Bian · Xiang Wei · Shan Deng ·
Qi-Zhu Tang · Jinghua Feng · Yan Zhang · Chen Liu ·
Ding-Sheng Jiang · Ling Yan · Lian-Feng Zhang ·
Manyin Chen · John Fassett · Yingjie Chen ·
You-Wen He · Qinglin Yang · Peter P. Liu · Hongliang Li**

**Abstract** Cardiac hypertrophy is a response of the myocardium to increased workload and is characterised by an increase of myocardial mass and an accumulation of extracellular matrix (ECM). As an ECM protein, an integrin ligand, and an angiogenesis inhibitor, all of which are key players in cardiac hypertrophy, mindin is an attractive target for therapeutic intervention to treat or prevent cardiac hypertrophy and heart failure. In this study, we investigated the role of mindin in cardiac hypertrophy using littermate *Mindin* knockout (*Mindin*$^{-/-}$) and wild-type (WT) mice. Cardiac hypertrophy was induced by aortic banding (AB) or angiotensin II (Ang II) infusion in *Mindin*$^{-/-}$ and WT

Bian Zhou-Yan, Xiang Wei and Shan Deng are as co-first authors.

**Electronic supplementary material** The online version of this article (doi:10.1007/s00109-012-0883-2) contains supplementary material, which is available to authorized users.

Z.-Y. Bian · Q.-Z. Tang · J. Feng · Y. Zhang · D.-S. Jiang ·
L. Yan · H. Li
Department of Cardiology, Renmin Hospital of Wuhan University,
JieFang Road 238,
Wuhan 430060, People's Republic of China

Z.-Y. Bian · Q.-Z. Tang · J. Feng · Y. Zhang · D.-S. Jiang ·
L. Yan · H. Li (✉)
Cardiovascular Research Institute of Wuhan University,
Wuhan 430060, People's Republic of China
e-mail: lihl@whu.edu.cn

X. Wei
Department of Thoracic and Cardiovascular Surgery,
Tongji Hospital, Tongji Medical College,
Huazhong University of Science and Technology,
Wuhan 430030, China

S. Deng
Department of Cardiology, Institute of Cardiovascular Disease,
Union Hospital, Tongji Medical College,
Huazhong University of Science and Technology,
Wuhan, China

C. Liu
Department of Cardiology, The First Affiliated Hospital,
Sun Yat-Sen University,
Guangzhou, China

L.-F. Zhang
Key Laboratory of Human Disease
Comparative Medicine, Ministry of Health,
Beijing, China

M. Chen · P. P. Liu
Division of Cardiology, Heart and Stroke/Richard Lewar Centre
of Excellence. University Health Network, University of Toronto,
Ontario M5S3E2, Canada

J. Fassett · Y. Chen
Cardiovascular Division, University of Minnesota,
Minneapolis, MN 55455, USA

Y.-W. He
Department of Immunology, Duke University Medical Center,
Durham, NC 27710, USA

Q. Yang
Department of Nutrition Sciences,
University of Alabama at Birmingham,
Birmingham, AL 35294-3360, USA

mice. The extent of cardiac hypertrophy was quantitated by echocardiography and by pathological and molecular analyses of heart samples. $Mindin^{-/-}$ mice were more susceptible to cardiac hypertrophy and fibrosis in response to AB or Ang II stimulation than wild type. Cardiac function was also markedly exacerbated during both systole and diastole in $Mindin^{-/-}$ mice in response to hypertrophic stimuli. Western blot assays further showed that the activation of AKT/glycogen synthase kinase 3β (GSK3β) signalling in response to hypertrophic stimuli was significantly increased in $Mindin^{-/-}$ mice. Moreover, blocking AKT/GSK3β signalling with a pharmacological AKT inhibitor reversed cardiac abnormalities in $Mindin^{-/-}$ mice. Our data show that mindin, as an intrinsic cardioprotective factor, prevents maladaptive remodelling and the transition to heart failure by blocking AKT/GSK3β signalling.

**Keywords** Mindin · Hypertrophy · Remodelling · Signal transduction · AKT

## Introduction

Cardiac hypertrophy is a response of the myocardium to increased workload and is characterised by an increase in myocardial mass and an accumulation of extracellular matrix (ECM) [1]. Although initial cardiac hypertrophy probably constitutes an adaptive mechanism, prolonged and severe hypertrophy is a risk factor for arrhythmias, sudden death and heart failure. The molecular mechanism that mediates the transition from hypertrophy to heart failure remains largely unknown. Accumulating evidence indicates that ECM proteins, such as fibronectin, osteopontin, melusin and laminin, play key roles in the progression of cardiac hypertrophy [1, 2]. Fibronectin induces cardiac myocyte hypertrophy in vitro [2]. Additionally, osteopontin and melusin are required to sustain compensatory cardiac hypertrophy in response to chronic pressure overload and prevent the transition toward HF [3]. However, laminin α4-deficient mice gradually develop cardiac hypertrophy with impaired function [4]. A balance seems to exist among the matrix proteins, and this balance regulates cardiac hypertrophy. Therefore, the discovery and functional clarification of novel cardiac hypertrophy-related ECM proteins is important for understanding the molecular mechanisms underlying cardiac hypertrophy.

Mindin is a member of the mindin/F-spondin family of secreted ECM proteins, which contain N-terminal F-spondin (FS) domains and C-terminal thrombospondin type 1 repeats (TSR). Mindin was originally discovered in zebrafish as a component of the basal lamina [5]. Subsequently, mindin was shown to promote the outgrowth of hippocampal embryonic neurons and to inhibit angiogenesis [5].

Recent studies have demonstrated that mindin serves as a ligand for integrins; specifically, the FS domain of mindin mediates integrin binding [5–7]. The mindin–integrin interactions are not only critical for recruiting inflammatory cells, such as neutrophils, macrophages and eosinophils, but also play a key role in regulating Rho GTPase expression in dendritic cells (DCs) and in DC priming of T lymphocytes [5–7]. Additionally, mindin functions as a pattern-recognition molecule for microbial pathogens via its TSR domain, which recognises pathogen-associated molecular patterns and is essential in the innate immune response [8]. To date, research on mindin has focused on infectious diseases and cancer [5–8]. Northern blot analysis of $Mindin$ expression in mouse tissues demonstrated that $Mindin$ is highly expressed in the heart [5]. As an ECM protein, an integrin ligand, and an angiogenesis inhibitor, all of which are key players in cardiac hypertrophy, mindin is an attractive target for therapeutic intervention to treat or prevent cardiac hypertrophy and heart failure. Most recently, we published our findings related to the mindin protein and discovered that cardiac-specific overexpression of human mindin protein protects against cardiac hypertrophy by blocking AKT signalling in mice [9]. However, these protective effects of mindin were mediated by exogenously expressed protein but not by endogenous mindin. To investigate accurately the critical role of mindin in the heart, we used $Mindin^{-/-}$ mice. Importantly, our new data demonstrated that disruption of mindin exacerbates cardiac hypertrophy and fibrosis by activation of AKT/GSK3β signalling.

## Methods and materials

### Materials

Primary antibodies against the following proteins were purchased from Santa Cruz Biotechnology: murine mindin (sc-49050), atrial natriuretic peptide (ANP; sc-20158), brain natriuretic peptide (BNP; sc-18817), β-MHC (sc-53090), Collagen I (sc-8784), Collagen III (sc-8781) and Lamin B1 (sc-6217). Antibodies against human mindin (ab70508) and CTGF (ab51704) were obtained from Abcam. Antibodies against phospho-JNK1/2$^{Thr183/Tyr185}$, FOXO1, phospho-FOXO1$^{Ser256}$, FOXO3A, phospho-FOXO3A$^{Ser318/321}$, Smad2, phospho-Smad2$^{Ser465/467}$, Smad3, phospho-Smad3$^{Ser423/425}$, Smad4 and GAPDH were purchased from Cell Signalling Technology. Antibodies against phospho-ERK1/2$^{Thr202/Tyr204}$, ERK1/2, JNK1/2, phospho-P38$^{Tyr182}$, P38, phospho-AKT$^{Thr308}$, AKT, phospho-GSK3β$^{Ser9}$, GSK3β, phospho-mTOR$^{Ser2448}$, mTOR and TGFβ1 were purchased from Bioworld Technology. The BCA protein assay kit was purchased from Pierce. IRDye® 800CW conjugated secondary antibodies

(LI-COR Biosciences) were used for visualisation. AKT Inhibitor IV (SC-203809) was ordered from Santa Cruz Biotechnology. All other reagents were obtained from Sigma.

## Animals and animal models

The study protocol was approved by the Animal Care and Use Committee of Renmin Hospital of Wuhan University, China. Male *Mindin* knockout mice (*Mindin*$^{-/-}$, C57BL/6 background) and their wild-type littermates (aged 7 to 8 weeks) were used in the studies. Genotyping was performed by PCR as described previously [8].

Aortic banding was performed as described previously [10, 11]. To confirm the role of mindin in cardiac hypertrophy, the experiments were repeated in an angiotensin II (Ang II) infusion model, which was established as described previously [12]. Ang II (1.4 mg kg$^{-1}$ day$^{-1}$ dissolved in 0.9% NaCl) was subcutaneously infused for 4 weeks using an osmotic minipump (Alzet model 2004; Alza Corp) implanted in each mouse. Saline-infused animals served as infusion controls and were subjected to the same procedures as the experimental animals, with the exception of the Ang II infusion. AKT Inhibitor IV (AKTI; 0.5 mg kg$^{-1}$ days$^{-1}$) suspension was freshly prepared and administered by intraperitoneal injection every 3 days. AKT inhibitor was administration 1 week before surgery and then continued for 4 weeks after aortic banding (AB) or sham. Mice in the control group received the same volume of PBS. The internal diameter and wall thickness of the left ventricle (LV) were assessed by echocardiography. Hearts, lungs, and tibiae of the sacrificed mice were dissected and weighed or measured to compare the heart weight (HW)/body weight (BW; in mg/g), HW/tibial length (TL; in mg/mm) and lung weight (LW)/BW (in mg/g) ratios in the different groups.

## Blood pressure and echocardiography

A microtip catheter transducer (SPR-839, Millar Instruments, Houston, Texas) was inserted into the right carotid artery and advanced into the left ventricle. The pressure signals and heart rate were recorded continuously using an ARIA pressure-volume conductance system coupled to a Powerlab/4SP A/D converter [10–12]. Echocardiography was performed via a MyLab 30CV ultrasound (Biosound Esaote Inc.) with a 10-MHz linear array ultrasound transducer. End-systole or end-diastole was defined as the phase in which the smallest or largest area of LV, respectively, was obtained. LV end-systolic diameter (LVESD) and LV end-diastolic diameter (LVEDD) were measured from the LV M-mode tracing with a sweep speed of 50 mm/s at the mid-papillary muscle level.

## Western blotting

Cardiac tissue was lysed in RIPA lysis buffer. Nuclear protein extracts were isolated as described previously [10–12]. Fifty micrograms of the protein extracts was used for SDS-PAGE. The proteins were then transferred to nitrocellulose membranes and probed with various antibodies. After incubation with a secondary IRDye® 800CW-conjugated antibody, the signals were visualised using an Odyssey Imaging System. Specific protein expression levels on the same nitrocellulose membrane were normalised to either GAPDH for the total cell lysate and cytosolic proteins or to lamin-B1 for nuclear proteins.

## Histological analysis

Hearts were excised, placed immediately in 10% potassium chloride solution to ensure that they were stopped in diastole, washed with saline solution, and placed in 10% formalin. Hearts sections (4–5 μm thick) were prepared and stained with hematoxylin–eosin (HE) for histopathology or Picrosirius red (PSR) for collagen deposition and then visualised by light microscopy. A single myocyte was measured using an image quantitative digital analysis system (Image-Pro Plus 6.0). Between 100 and 200 myocytes in the left ventricles were outlined in each group.

## Immunohistochemistry

Immunohistochemistry was undertaken to localise the phosphorylated Akt and Smad2/3 in cardiomyocytes and interstitium. Perfusion-fixed (4% paraformaldehyde), paraffin-embedded sections of *Mindin*$^{+/+}$ and *Mindin*$^{-/-}$ mice 4 weeks after AB surgery were stained using the antibodies against phospho-AKT$^{Thr308}$, phospho-Smad2$^{Ser465/467}$, or phospho-Smad3$^{Ser423/425}$, developed with peroxidase-coupled secondary antibodies and DAB as a substrate. Images were captured at 400x magnification from 5 fields /case. The positive areas of the histological sections were quantified using an image quantitative digital analysis system (Image-Pro Plus 6.0).

## Statistical analysis

Data are expressed as means±SEM. Differences among groups were determined by two-way ANOVA followed by a *post hoc* Tukey test. Comparisons between two groups were performed using an unpaired Student's *t* test. A value of $P < 0.05$ was considered significant.

## Results

### Mindin expression in experimental hypertrophic models

To explore the potential role of mindin in cardiac hypertrophy, we first analysed mindin expression in well-established models of cardiac hypertrophy induced by pressure overload or chronic infusion of Ang II. As shown in Fig. 1, mindin protein levels were gradually and significantly increased in the LV of mice subjected to AB or Ang II infusion during the first 2 weeks. However, mindin expression markedly decreased at week 4. In addition, protein levels of hypertrophic markers, such as ANP and BNP, were elevated in a time-dependent manner from weeks 1 to 4 following AB or Ang II infusion (Fig. 1). Thus, these findings imply a compensatory increase of mindin expression in adaptive cardiac hypertrophy (the first 2 weeks following hypertrophic stimuli) and a subsequent decompensatory decrease in mindin expression during maladaptive remodelling (the final 2 weeks).

### Mindin$^{-/-}$ mice are more susceptible to cardiac hypertrophy in response to pressure overload or Ang II stimulation

To examine the role of mindin in the heart, we used Mindin$^{-/-}$ mice that lack mindin protein expression in the heart (Fig. 2a). Under basal conditions, mindin deficiency had no significant effect on HW/BW, LW/BW or LV dimensions; wall thickness; or LV function (evaluated by echocardiographic parameters such as LVEDD, LVESD, PWT, IVSD and FS) compared with Mindin$^{+/+}$ mice (Table 1). This finding suggests that mindin plays a negligible role in cardiac development or function under basal conditions.

To investigate the role of mindin in cardiac hypertrophy, Mindin$^{-/-}$ mice and Mindin$^{+/+}$ littermate control mice were subjected to AB surgery or sham surgery. Four weeks following AB surgery, the Mindin$^{+/+}$ mice exhibited cardiac hypertrophy, as evidenced by increased HW/BW, HW/TL and cross-sectional area of cardiac myocytes (Fig. 2b). Importantly, increased hypertrophy was observed in Mindin$^{-/-}$ mice compared with Mindin$^{+/+}$ controls (Fig. 2b). It is necessary to produce equal aortic banding in different groups, which showed similar pressure overload to compare the effect of mindin. We detected a similar systolic blood pressure of 150–160 mmHg in the LV after 4 weeks of AB among groups by microtip catheter transducer (Table 2). Cardiac hypertrophy and function were examined by echocardiography 4 weeks after surgery. The increase in LV dimensions and wall thickness demonstrated that the left ventricular dilation was significant in Mindin$^{-/-}$ mice compared with their Mindin$^{+/+}$ littermates according to echocardiographic parameters, such as LVEDD, LVESD, PWT and IVSD (Table 2). The decreased FS and EF and the increased lung weight demonstrated the exacerbated LV function in Mindin$^{-/-}$ mice compared with their Mindin$^{+/+}$ littermates (Table 2; Fig. 2b). We also conducted serial echocardiography to observe the phenotypic changes in Mindin$^{-/-}$ mice 1–2 weeks after AB to track the effects of mindin on cardiac dysfunction. The knockout animals demonstrated a significant increase in left ventricular chamber size and decrease in systolic function, which was consistent with maladaptive cardiac remodelling. This difference reached statistical significance over the time period studied (Table 1 in the Electronic supplementary material). These results suggest that mindin is essential for the preservation of cardiac function over time. Likewise, histological



Fig. 1 Mindin expression in experimental hypertrophic models. *Top*, Representative Western blots for mindin, ANP and BNP in experimental hypertrophic models induced by aortic banding or Ang II infusion at the indicated time points. *Bottom*, quantitative results of the protein levels of mindin, ANP and BNP in heart tissue after AB or Ang II infusion at the indicated time points. $*P < 0.01$ was obtained for the sham group
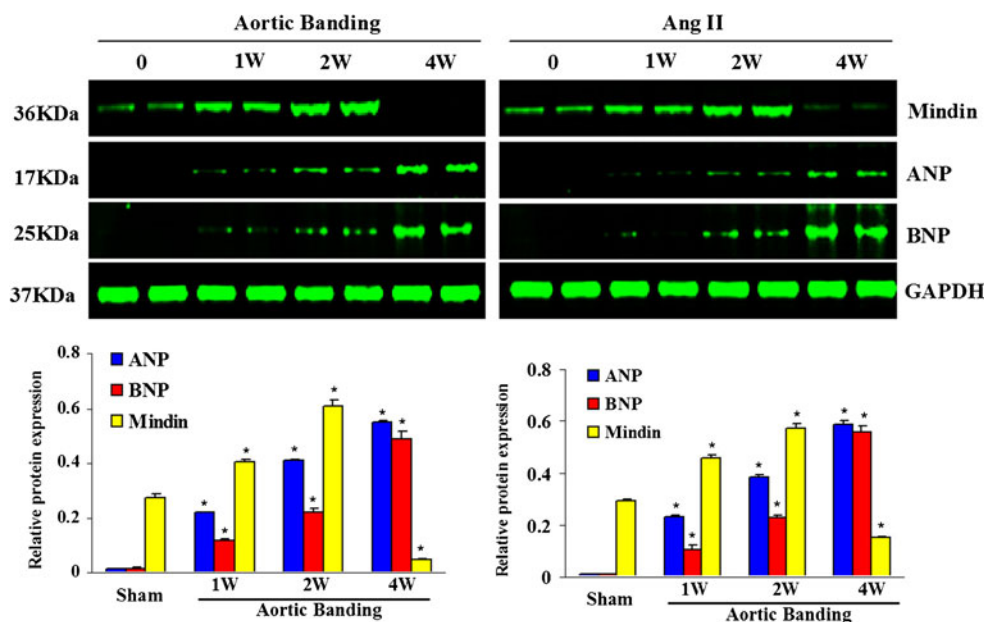
**Fig. 2** *Mindin*$^{-/-}$ mice are more susceptible to cardiac hypertrophy in response to pressure overload or Ang II stimulation. **a** Representative Western blots for murine mindin in heart tissue from *Mindin*$^{+/+}$ and *Mindin*$^{-/-}$ mice (*n*=4). **b**, **d** Statistical results for HW/BW, HW/TL and LW/BW ratios and myocyte cross-sectional areas (*n*=100 cells/group) 4 weeks after AB surgery (**b**) or Ang II infusion (**d**) in *Mindin*$^{+/+}$ and *Mindin*$^{-/-}$ mice (*n*=5–6 mice/group). **c**, **e** Gross hearts, whole hearts and HE staining 4 weeks after AB surgery (**c**) or Ang II infusion (**e**) in *Mindin*$^{+/+}$ and *Mindin*$^{-/-}$ mice. *Scale bars*, gross heart= 20 mm; HE staining=50 μm. **f**, **g** Protein expression levels of ANP, BNP and β-MHC 4 weeks after AB surgery (**f**) or Ang II infusion (**g**) in *Mindin*$^{+/+}$ and *Mindin*$^{-/-}$ mice (*n*=4). *Left*, representative blots; *right*, quantitative results. *$P$<0.01 for *Mindin*$^{+/+}$/sham or *Mindin*$^{+/+}$/saline values; †$P$<0.01 for *Mindin*$^{+/+}$/AB or *Mindin*$^{+/+}$/ Ang II after AB or Ang II infusion
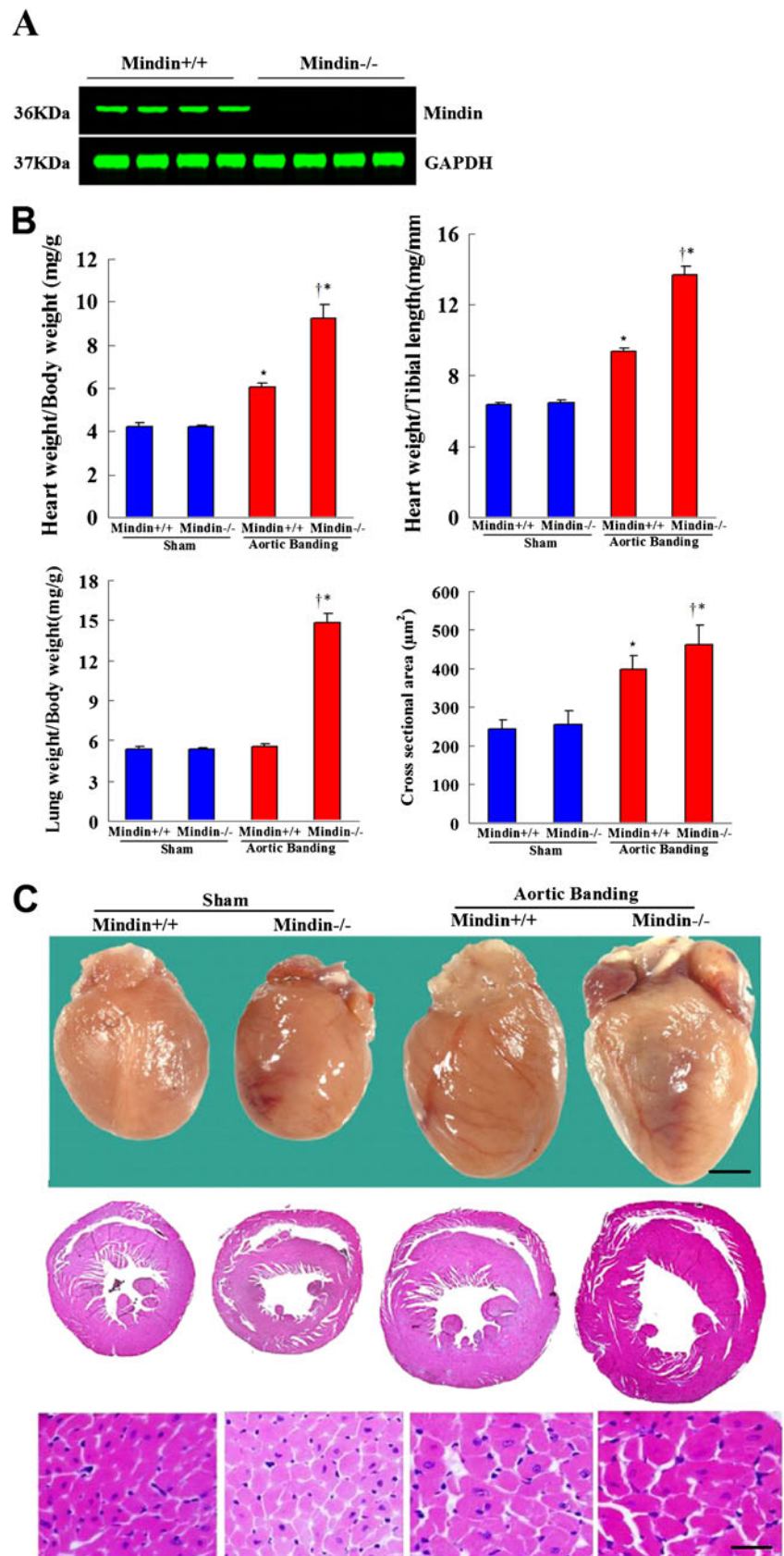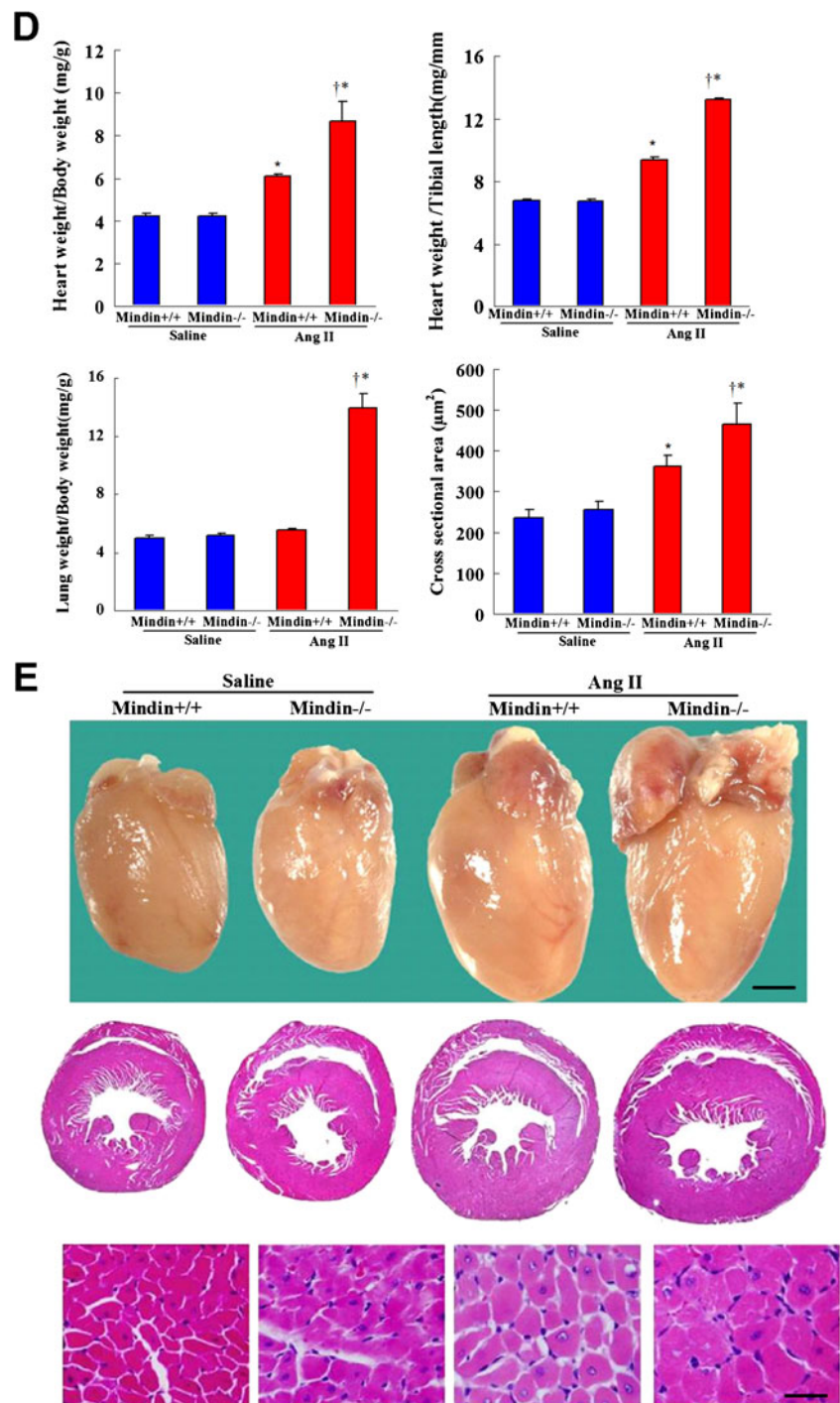
**Fig. 2** (continued)



analyses based on gross and whole-heart examinations and HE staining revealed the exaggerated effect of mindin deficiency on cardiac hypertrophy in response to pressure overload (Fig. 2c). To examine these findings further, we established an Ang II-induced cardiac hypertrophy model in *Mindin*$^{-/-}$ and *Mindin*$^{+/+}$ mice. Using this model, we observed results similar to those obtained with AB treatment (Fig. 2d, e; Table 3). Additionally, we analysed the expression of several cardiac hypertrophy markers in response to pressure overload or Ang II stimulation. The protein levels of ANP, BNP and β-myosin heavy chain (β-MHC) were markedly elevated in both *Mindin*$^{-/-}$ and *Mindin*$^{+/+}$ mice after AB or Ang II infusion. Furthermore, these increases were more pronounced in *Mindin*$^{-/-}$ than in *Mindin*$^{+/+}$ mice 4 weeks after AB or Ang II infusion (Fig. 2f, g). These findings suggest that mindin protects against cardiac hypertrophy in response to pressure overload or Ang II stimulation.

**Fig. 2** (continued)
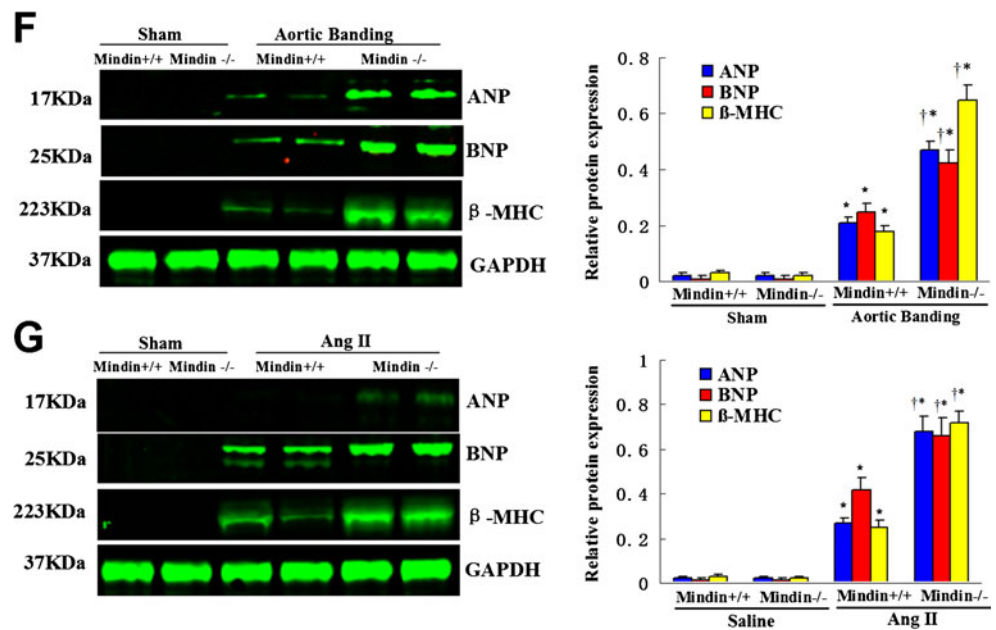


Mindin suppresses AKT/GSK3β signalling in response to pressure overload or Ang II stimulation

To explore the molecular mechanisms by which mindin inhibits the hypertrophic response, we examined the effects of mindin on MAPK signalling. We found that the phosphorylated levels of ERK1/2, JNK1/2 and p38 were significantly increased in both AB and Ang II-infused $Mindin^{+/+}$ hearts. However, these phosphorylation levels were not significantly different between $Mindin^{-/-}$ and $Mindin^{+/+}$ hearts (Fig. 3a). These data imply that the antihypertrophic effects of mindin are not due to modulation of the MAPK pathway. To further determine whether mindin blocks AKT/

GSK3β signalling in response to hypertrophic stimuli, we examined AKT/GSK3β activation between $Mindin^{+/+}$ and $Mindin^{-/-}$ mice. Our results demonstrated that mindin deficiency markedly enhanced AKT and GSK3β phosphorylation induced by AB or Ang II infusion (Fig. 3b). The immunostaining of the cardiac sections also indicated that the phosphorylation of AKT in cardiomyocytes was significantly increased in $Mindin^{-/-}$ mice compared with $Mindin^{+/+}$ controls (Fig. 3c). The phosphorylated levels of mammalian target of rapamycin (mTOR), forkhead box O3A (FOXO3A) and forkhead box O1 (FOXO1) were also increased in $Mindin^{-/-}$ mice, although the total levels of these kinases were unchanged, which is consistent with upregulation of the AKT pathway (Fig. 3b).

Mindin protects against fibrosis in response to pressure overload or Ang II stimulation

Pathological cardiac hypertrophy is associated with increased fibrosis of the myocardium [11]. To investigate further the mechanisms by which mindin suppresses maladaptive remodelling in response to hypertrophic stress, we examined the ability of mindin to suppress fibrosis. As shown in Fig. 4a, increased collagen deposition was observed in the $Mindin^{+/+}$ mice subjected to AB or Ang II infusion, but this was markedly increased in $Mindin^{-/-}$ mice. Quantitative analysis also showed enhanced collagen volume in the myocardium of $Mindin^{-/-}$ mice compared with $Mindin^{+/+}$ mice (Fig. 4b). Subsequent analyses of protein expression levels of known mediators of fibrosis, including connective tissue growth factor (CTGF), collagen I, collagen III, and transforming growth factor (TGF)-β1, revealed a pronounced fibrotic response in $Mindin^{-/-}$ mice

**Table 1** Anatomic and echocardiographic analysis in 10- to 12-week-old mice

| Parameter | $Mindin^{-/-}$ mice | $Mindin^{+/+}$ mice |
|---|---|---|
| Number | 8 | 8 |
| BW (g) | 25.72±0.39 | 25.74±0.41 |
| HW/BW | 3.66±0.07 | 3.63±0.12 |
| LW/BW | 3.90±0.10 | 3.94±0.13 |
| HW/TL | 6.14±0.13 | 6.12±0.14 |
| HR (beats/min) | 509.83±8.72 | 488.22±17.56 |
| LVEDD (mm) | 3.80±0.02 | 3.74±0.04 |
| LVESD (mm) | 1.80±0.01 | 1.78±0.02 |
| IVSD (mm) | 0.75±0.03 | 0.71±0.04 |
| FS (%) | 52.47±0.48 | 52.37±0.75 |

*HR* heart rate, *BW* body weight, *HW* heart weight, *TL* tibial length, *LVEDD* left ventricular end-diastolic diameter, *LVESD* left ventricular end-systolic diameter, *PWT* posterior wall thickness, *IVSD* left ventricular septum, diastolic, *FS* fractional shortening. All values are mean± SEM

**Table 2** Echocardiographic and haemodynamics parameters in *Mindin*$^{-/-}$ and *Mindin*$^{+/+}$ mice at 4 weeks after sham operation or AB

| Parameter | Sham *Mindin*$^{+/+}$ mice | Sham *Mindin*$^{-/-}$ mice | AB *Mindin*$^{+/+}$ mice | AB *Mindin*$^{-/-}$ mice |
|---|---|---|---|---|
| Number | 8 | 9 | 8 | 9 |
| BW (g) | 27.55±0.56 | 28.46±0.61 | 28.28±0.41 | 27.84±0.64 |
| HR (beats/min) | 478.41±6.43 | 478.10±16.25 | 480.60±13.44 | 546.90±12.19 |
| LVEDD (mm) | 3.53±0.04 | 3.70±0.02 | 4.38±0.09* | 5.21±0.07*, ** |
| LVESD (mm) | 1.62±0.03 | 1.73±0.02 | 2.46±0.08* | 3.50±0.06*, ** |
| IVSD (mm) | 0.62±0.02 | 0.59±0.02 | 0.80±0.02 | 1.08±0.05* |
| FS (%) | 54.08±1.14 | 53.29±0.63 | 43.57±2.05* | 32.65±1.77*, ** |
| SBP (mmHg) | 112.7±4.9 | 110.2±2.8 | 157.3±5.4* | 150.7±6.2* |
| EF (%) | 61.7±5.5 | 56.3±5.6 | 35.7±3.1* | 24.1±2.6*, ** |
| LVEDP (mmHg) | 9.3±1.1 | 9.7±1.6 | 16.9±2.5* | 23.4±1.5** |
| LV $dP/dT_{max}$ (mmHg/s) | 8,738.7±567.7 | 8,894.7±588.5 | 7,423.6±403.2* | 6,225.2±419.8** |
| LV $dP/dT$min (mmHg/s) | −8,115.7±534.9 | −8,251.9±566.1 | −6,855.8±511.4* | −5,339.3±442.3** |

All values are mean±SEM

*$P<0.05$ versus *Mindin*$^{+/+}$ sham operation; **$P<0.05$ versus *Mindin*$^{+/+}$ AB after 4 weeks AB

(Fig. 4c). To elucidate further the molecular mechanisms underlying the antifibrotic effects of mindin, we assessed the regulatory role of mindin in Smad activation, which plays a crucial role in fibrosis [12]. We found that *Mindin*$^{-/-}$ mice exhibited higher levels of Smad2 phosphorylation and greater nuclear translocation of Smad2/3 compared with *Mindin*$^{+/+}$ mice (Fig. 4d). The immunohistological staining of the cardiac sections also showed that the phosphorylation, the nuclear translocation of Smad2/3 in cardiomyocytes, and the interstitial were significantly increased in *Mindin*$^{-/-}$ mice compared with *Mindin*$^{+/+}$ controls (Fig. 4e). These results suggest that mindin protects against fibrosis by blocking Smad signalling.

Blocking AKT/GSK3β signalling reverses cardiac abnormalities in *Mindin*$^{-/-}$ mice

The above results suggest that mindin suppresses cardiac hypertrophy and fibrosis through the blockade of AKT/GSK3β and TGF-β1 signalling pathways. To further examine these findings, we evaluated whether the abnormalities in *Mindin*$^{-/-}$ mice could be reversed by blocking AKT/GSK3β signalling with a pharmacological agent, AKTI, in vivo. Therefore, we treated *Mindin*$^{-/-}$ mice with AKTI or PBS following AB. Western blot analysis revealed that the phosphorylation levels of AKT and GSK3β were almost completely abrogated in samples from AKTI-treated mice compared with PBS-treated control mice (Fig. 5a, b). Next, we studied the effects of AKT/GSK3β signalling inhibition on cardiac remodelling. We examined the effects of the AKT inhibitor in WT mice subjected to aortic banding for 4 weeks. The results showed that the AKT inhibitor blocked cardiac hypertrophy mediated by 4 weeks of long-term pressure overload (Table 2 in the Electronic supplementary material).We further found that compared with PBS treatment, AKTI treatment significantly reversed the detrimental effects of 4-week AB on cardiac mass, function, morphology and hypertrophic marker expression in *Mindin*$^{-/-}$ mice (Fig. 5c–e; Table 4). These results suggest

**Table 3** Echocardiographic and haemodynamics parameters in *Mindin*$^{-/-}$ and *Mindin*$^{+/+}$ mice at 4 weeks after Ang II or saline infusion

| Parameter | Saline *Mindin*$^{+/+}$ mice | Saline *Mindin*$^{-/-}$ mice | Ang II *Mindin*$^{+/+}$ mice | Ang II *Mindin*$^{-/-}$ mice |
|---|---|---|---|---|
| Number | 8 | 9 | 8 | 9 |
| BW (g) | 29.54±0.68 | 29.46±0.70 | 28.49±0.59 | 28.02±0.58 |
| HR (beats/min) | 500.93±8.92 | 511.17±11.19 | 500.17±9.72 | 499.75±13.81 |
| LVEDD (mm) | 3.57±0.05 | 3.69±0.05 | 4.28±0.11* | 5.03±0.07*, ** |
| LVESD (mm) | 1.59±0.02 | 1.69±0.02 | 2.34±0.06* | 3.26±0.10*, ** |
| IVSD (mm) | 0.65±0.01 | 0.54±0.01 | 0.82±0.05 | 0.95±0.04* |
| FS (%) | 53.70±1.14 | 54.18±0.73 | 45.19±1.58* | 35.33±1.41*, ** |
| SBP (mmHg) | 107.5±4.5 | 110.7±3.9 | 143.7±4.4* | 141.8±4.2* |
| EF (%) | 58.2±3.8 | 56.7±5.1 | 44.6±5.6* | 32.7±2.6*, ** |
| LVEDP (mmHg) | 9.6±1.2 | 9.8±1.0 | 15.6±1.4* | 19.7±1.4** |
| LV $dP/dT_{max}$ (mmHg/s) | 8,567.4±435.1 | 8,665.5±408.5 | 7,003.7±433.6* | 6,145.1±454.7** |
| LV $dP/dT_{min}$ (mmHg/s) | −8,033.7±464.1 | −8,110.4±500.6 | −6,352.7±409.5* | −5,549.3±486.8** |

All values are mean±SEM

*$P<0.05$ versus *Mindin*$^{+/+}$ saline infusion; **$P<0.05$ versus *Mindin*$^{+/+}$ Ang II infusion after 4 weeks Ang II infusion

Fig. 3 Mindin suppresses AKT/GSK3β/mTOR/FOXO signalling in response to pressure overload or Ang II stimulation. a Representative blots for ERK1/2, JNK1/2 and p38 phosphorylation levels and their total protein expression levels 4 weeks after AB surgery or Ang II infusion in $Mindin^{+/+}$ and $Mindin^{-/-}$ mice ($n=4$). b Representative blots for AKT, GSK3β mTOR, FOXO3A and FOXO1 phosphorylation levels and their total protein expression levels 4 weeks following AB surgery or Ang II infusion in $Mindin^{+/+}$ and $Mindin^{-/-}$ mice ($n=4$). c Immunostaining for phosphorylated AKT 4 weeks after AB surgery in $Mindin^{+/+}$ and $Mindin^{-/-}$ mice. All images are representative of five similar experiments. Left, representative images; right, quantitative results. The ratios of p-AKT-positive areas of the histological sections were quantified using an image analysis system. *$P<0.01$ for $Mindin^{+/+}$ after AB
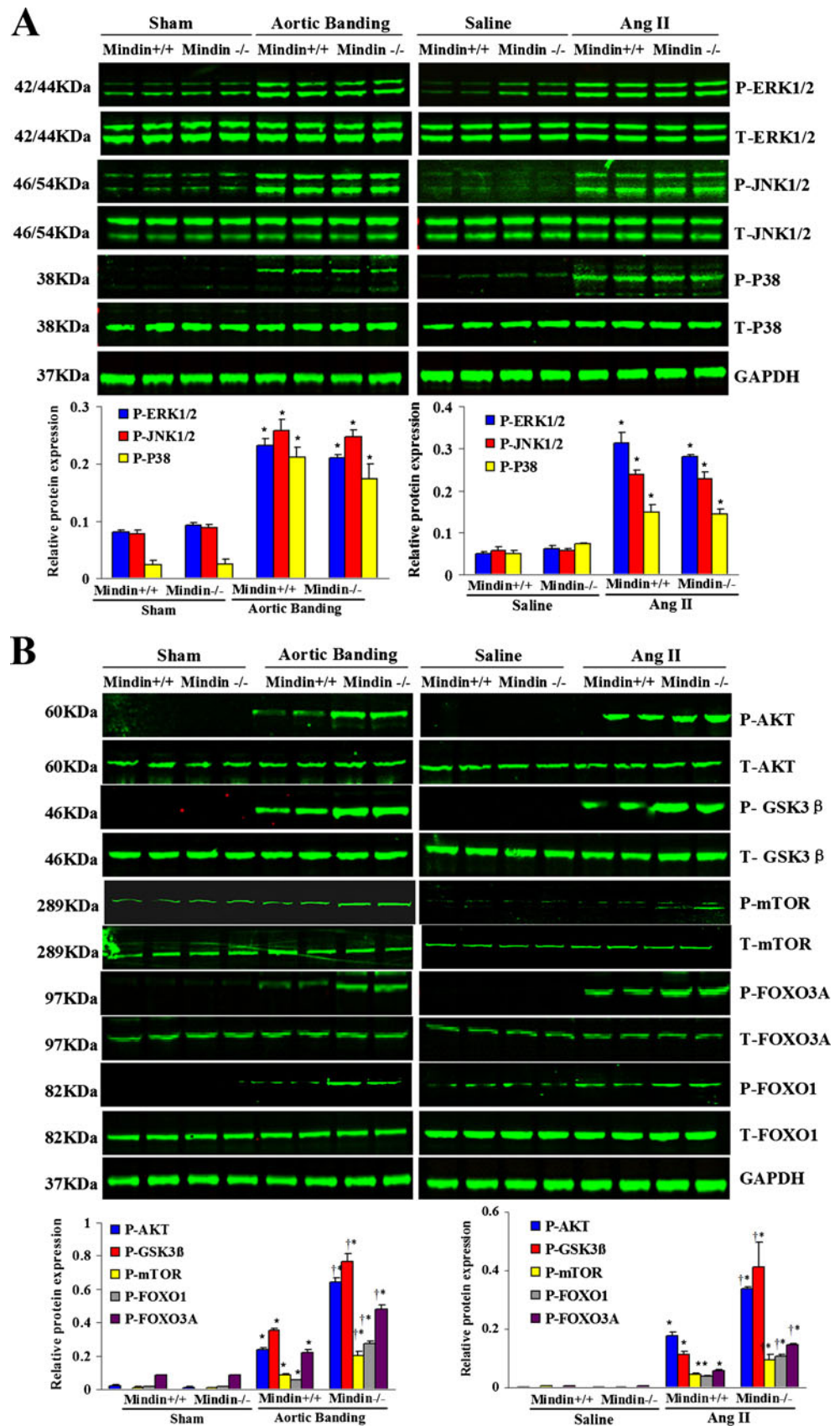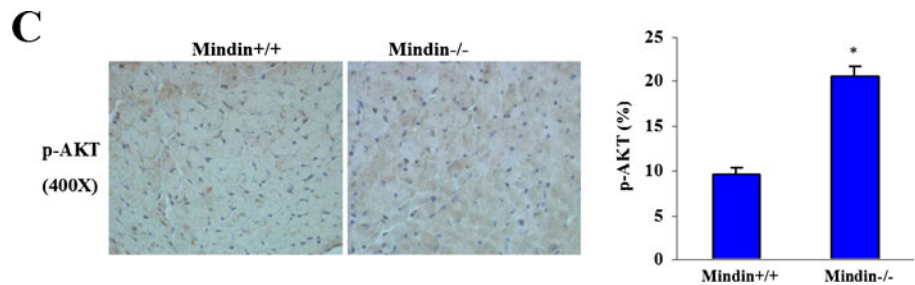
**Fig. 3** (continued)



that the inhibition of AKT/GSK3β signalling reverses cardiac hypertrophy in *Mindin*$^{-/-}$ mice. We next assessed whether the blockade of AKT/GSK3β signalling would affect the accelerated fibrosis observed in *Mindin*$^{-/-}$ mice. We found that AKTI treatment significantly reversed fibrosis, as evidenced by a decrease in the LV collagen volume and in the protein expression of fibrotic markers and diminished Smad2 phosphorylation and Smad2/3 nuclear translocation (Fig. 5f–h). Collectively, these findings indicate that pharmacological inhibition of AKT/GSK3β signalling rescues both cardiac hypertrophy and fibrosis in *Mindin*$^{-/-}$ mice in response to pressure overload.

**Discussion**

Mindin is a secreted extracellular matrix protein, an integrin ligand and an angiogenesis inhibitor, all of which are potential key players in the progression of cardiac hypertrophy. However, mindin's function during cardiac hypertrophy remains unclear. Recently, using cardiac-specific transgenic mice, we demonstrated that forced expression of the human mindin protein protects against cardiac hypertrophy by blocking AKT signalling in mice [9]. These protective roles of mindin were mediated by exogenously expressed protein. To reveal accurately the key role of mindin in cardiac remodelling, we used *Mindin*$^{-/-}$ mice. In this study, we demonstrated that disruption of mindin exacerbates cardiac remodelling by activating AKT/GSK3β signalling (Fig. 6).

Cardiac hypertrophy is part of a compensatory response to mechanical loading and neuro-hormonal signals. With persistent stress, however, the compensatory hypertrophy can evolve into a decompensated state with profound changes in gene expression, contractile dysfunction and extracellular remodelling [1]. The molecular mechanism that mediates the critical transition from compensated hypertrophy to decompensated HF remains elusive. Accumulating evidence indicates that ECM proteins, such as fibronectin, osteopontin, melusin and laminin, play key roles in the progression of cardiac hypertrophy [1–3]. In the present study, we identified mindin, a secreted ECM protein, as another intrinsic negative regulator of hypertrophy.

Mindin expression was increased during adaptive hypertrophy and markedly decreased during maladaptive cardiac remodelling. Moreover, *Mindin*$^{-/-}$ mice were more susceptible to cardiac hypertrophy in response to chronic pressure overload or Ang II stimulation. Notably, unlike osteopontin and melusin, which regulate hypertrophy induced only by mechanical stimuli [1–3], mindin can modulate hypertrophy induced by both mechanical and humoral stimuli, indicating a more potent function of mindin in hypertrophy. Together, these findings suggest that mindin may play a critical role in preventing cardiac hypertrophy and progression to HF.

To investigate the molecular mechanism by which mindin mediates its antihypertrophic effect, we examined the AKT signalling pathway, a pivotal contributor to the development of cardiac hypertrophy, as evidenced by our previous studies and others [13–20]. The downstream targets of AKT include GSK3β, mTOR and FOXO transcription factors, all of which are involved in cardiac hypertrophy. In the present study, AKT phosphorylation in response to hypertrophic stimuli was significantly increased in *Mindin*$^{-/-}$ mice. Consistent with the observed increase in AKT activity, hypertrophic stimuli resulted in increased levels of phosphorylation of GSK3β$^{Ser9}$ and FOXO transcription factors at AKT phosphorylation sites (reducing their anti-hypertrophic effects) and increased activation of mTOR in *Mindin*$^{-/-}$ mice compared with *Mindin*$^{+/+}$ mice. Moreover, blocking AKT/GSK3β signalling with a pharmacological AKT inhibitor reversed cardiac hypertrophy in *Mindin*$^{-/-}$ mice. Additionally, phosphorylation of ERK1/2, JNK1/2 and p38 MAPK was not significantly affected by mindin expression. Therefore, AKT/GSK3β signalling is a critical pathway through which mindin influences cardiomyocyte growth. In accordance with our findings, F-spondin, another member of the mindin/F-spondin family, inhibits the activation of AKT but not ERK1/2 or p38 when HUVECs grown on vitronectin are stimulated with VEGF [21]. Likewise, other researchers reported the requirement of AKT/GSK3β signalling for osteopontin and melusin to sustain compensatory cardiac hypertrophy in response to chronic pressure overload [1–3]. Some groups have reported that cardiac-specific overexpression of activated AKT induces cardiac hypertrophy and promotes fibrosis [22, 23]. In
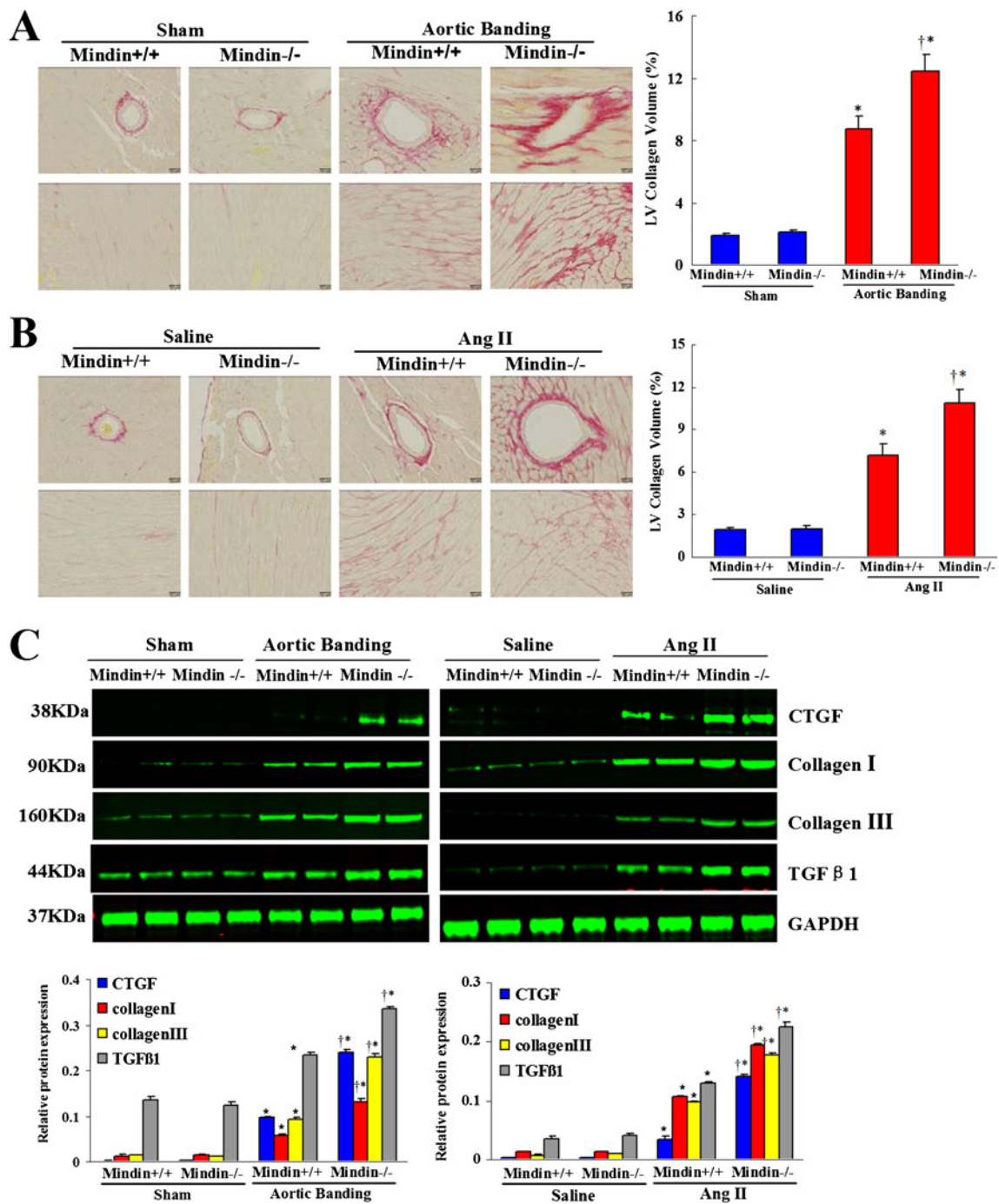
**Fig. 4** Mindin protects against fibrosis in response to pressure overload or Ang II stimulation. **a**, **b** Histological sections of the left ventricles of $Mindin^{+/+}$ and $Mindin^{-/-}$ mice ($n=6$) were stained with picrosirius red at 4 weeks after AB surgery (**a**) or Ang II infusion (**b**). *Left*, representative images; *right*, quantitative results; *scale bar*, 32 μm. Fibrotic areas of the histological sections were quantified using an image analysis system. *$P$ <0.01 for $Mindin^{+/+}$/sham or $Mindin^{+/+}$/saline values; †$P$<0.01 for $Mindin^{+/+}$/AB or $Mindin^{+/+}$/Ang II after AB or Ang II infusion. **c** Representative Western blots for CTGF, collagen I, collagen III and TGF-β1 4 weeks after AB surgery or Ang II infusion in $Mindin^{+/+}$ and $Mindin^{-/-}$ mice ($n=4$). **d** Representative blots for Smad2 phosphorylation and Smad2/3/4 translocation 4 weeks after AB surgery or Ang II infusion in $Mindin^{+/+}$ and $Mindin^{-/-}$ mice ($n=4$). **e** Immunostaining of p-Smad2 (*top*) and p-Smad3 (*bottom*) 4 weeks after AB surgery in $Mindin^{+/+}$ and $Mindin^{-/-}$ mice. All images are representative of five similar experiments. *Left*, representative images; *right*, quantitative results. The ratios of p-Smad2- and p-Smad3-positive areas of the histological sections were quantified using an image analysis system. *$P$<0.01 for $Mindin^{+/+}$ after AB

these studies, AKT-induced cardiac hypertrophy is associated with an increase in cardiomyocyte cell size and the activation of downstream AKT targets. However, there are also some differences in the results of the animal studies.
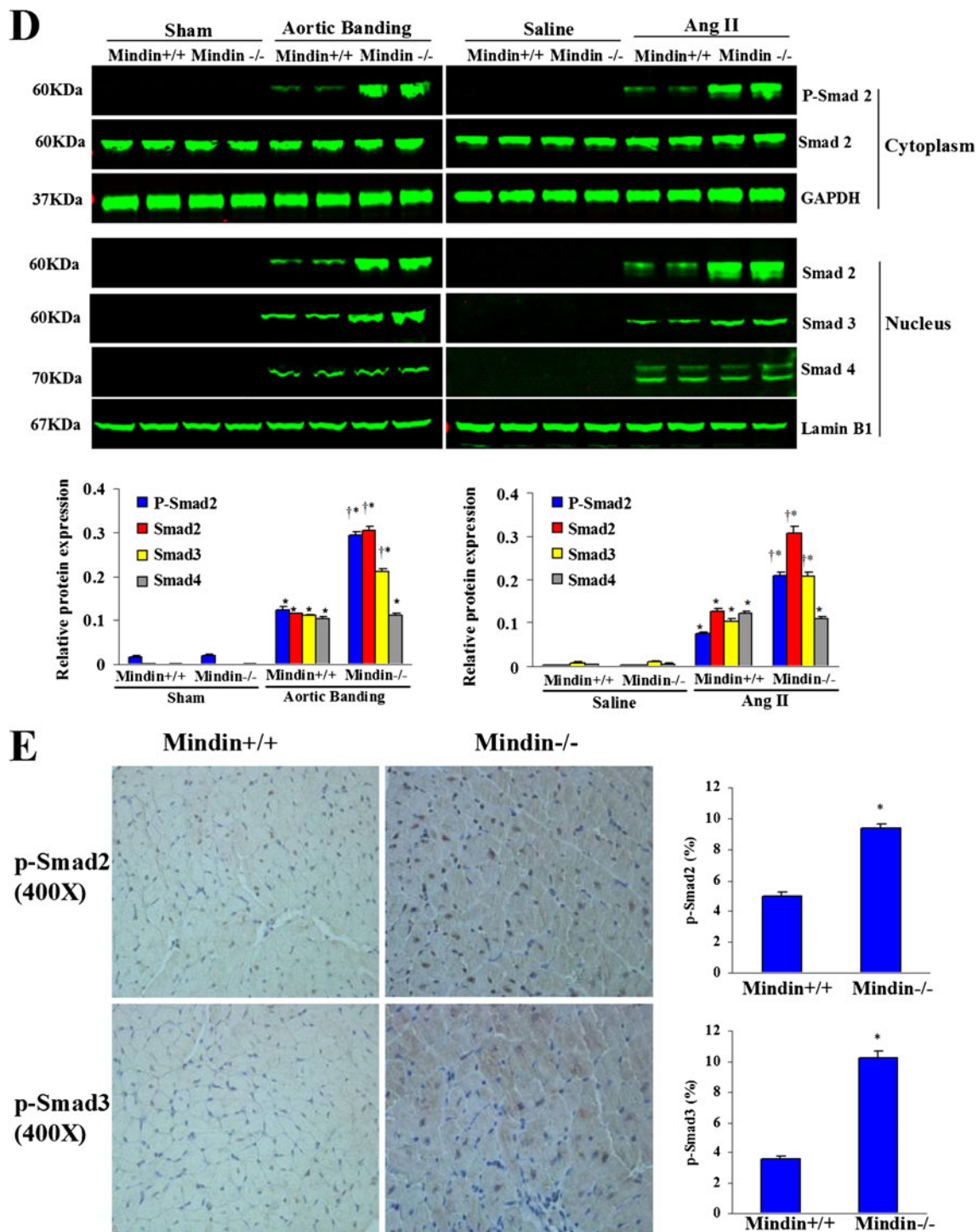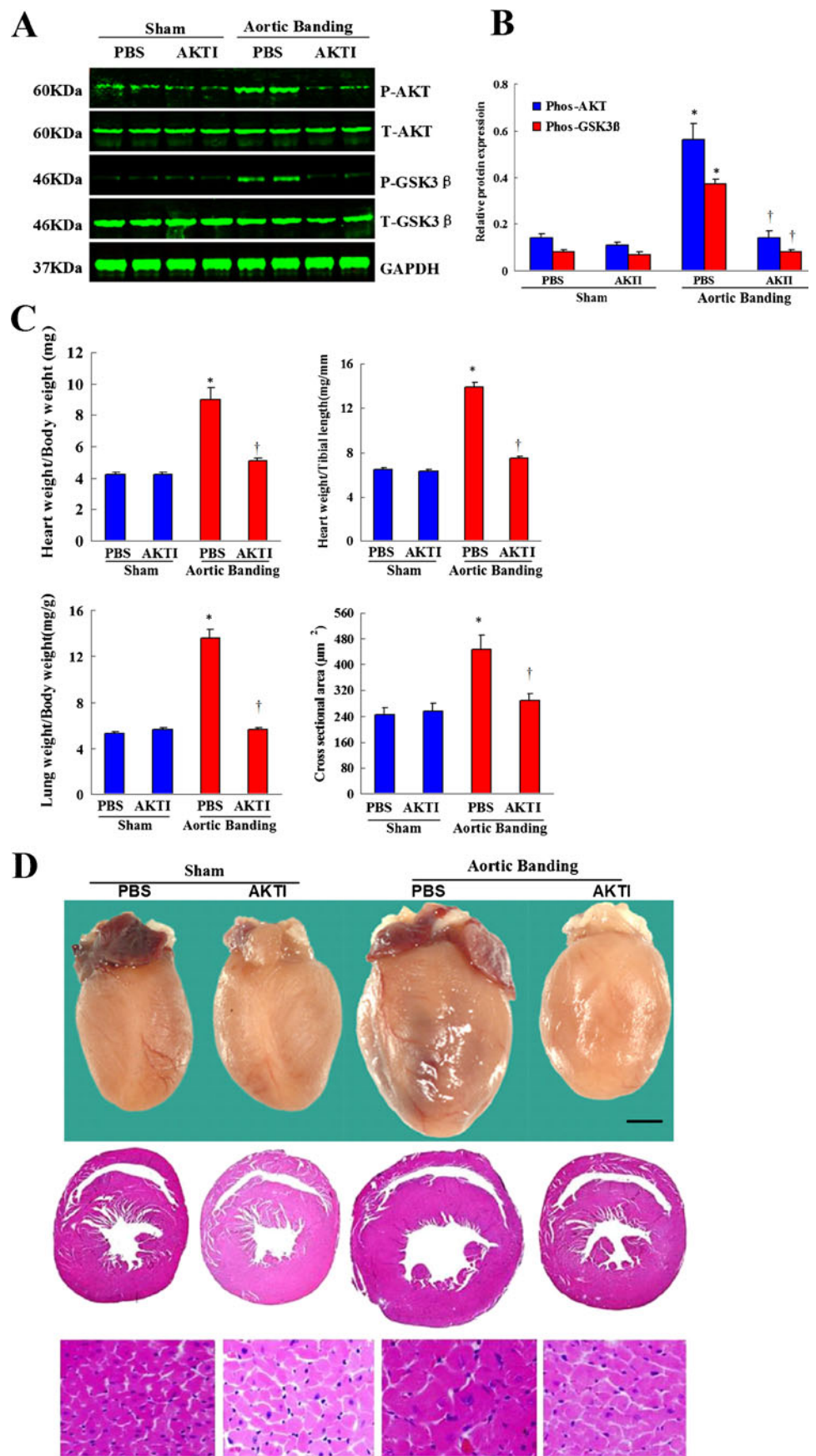
**Fig. 4** (continued)

Overexpression of the E40K mutant of AKT1 results in mild hypertrophy and enhanced contractility without signs of cardiac pathology [24]. In contrast, overexpression of myristoylated or phosphomimetic forms of AKT1 leads to a massive increase in heart size associated with impaired contractile function and interstitial fibrosis [22, 23].

Cardiac-specific expression of myristoylated AKT3 leads to cardiac growth that resembles compensated hypertrophy at 4 weeks of age but pathological hypertrophy at later ages [25]. Shiojima et al. [19] reported that short-term AKT activation induces "physiological" hypertrophy with a moderate increase in heart size, whereas prolonged AKT

Fig. 5 Blocking AKT/GSK3β signalling reverses cardiac abnormalities in *Mindin*$^{-/-}$ mice. **a**, **b** AKTI blocks AKT and GSK3β phosphorylation mediated by AB in *Mindin*$^{-/-}$ mice. **a** Representative blots; **b** quantitative results. **c** Effects of AKTI on HW/BW, HW/TL, LW/BW and cardiomyocyte cross-sectional area 4 weeks after AB. **d** Effects of AKTI on histological changes 4 weeks after surgery. **e** Effects of AKTI on hypertrophic markers of protein expression induced by AB. *Left*, representative blots; *right*, quantitative results. **f** Effects of AKTI on fibrosis. *Left*, PSR staining; *right*, statistical results for the fibrotic areas. **g** Effects of AKTI on fibrotic marker protein expression. **h** Effects of AKTI on Smad2 phosphorylation and Smad2/3/4 translocation. *$P$< 0.01 for PBS/sham values; †$P$< 0.01 for PBS/AB after AB
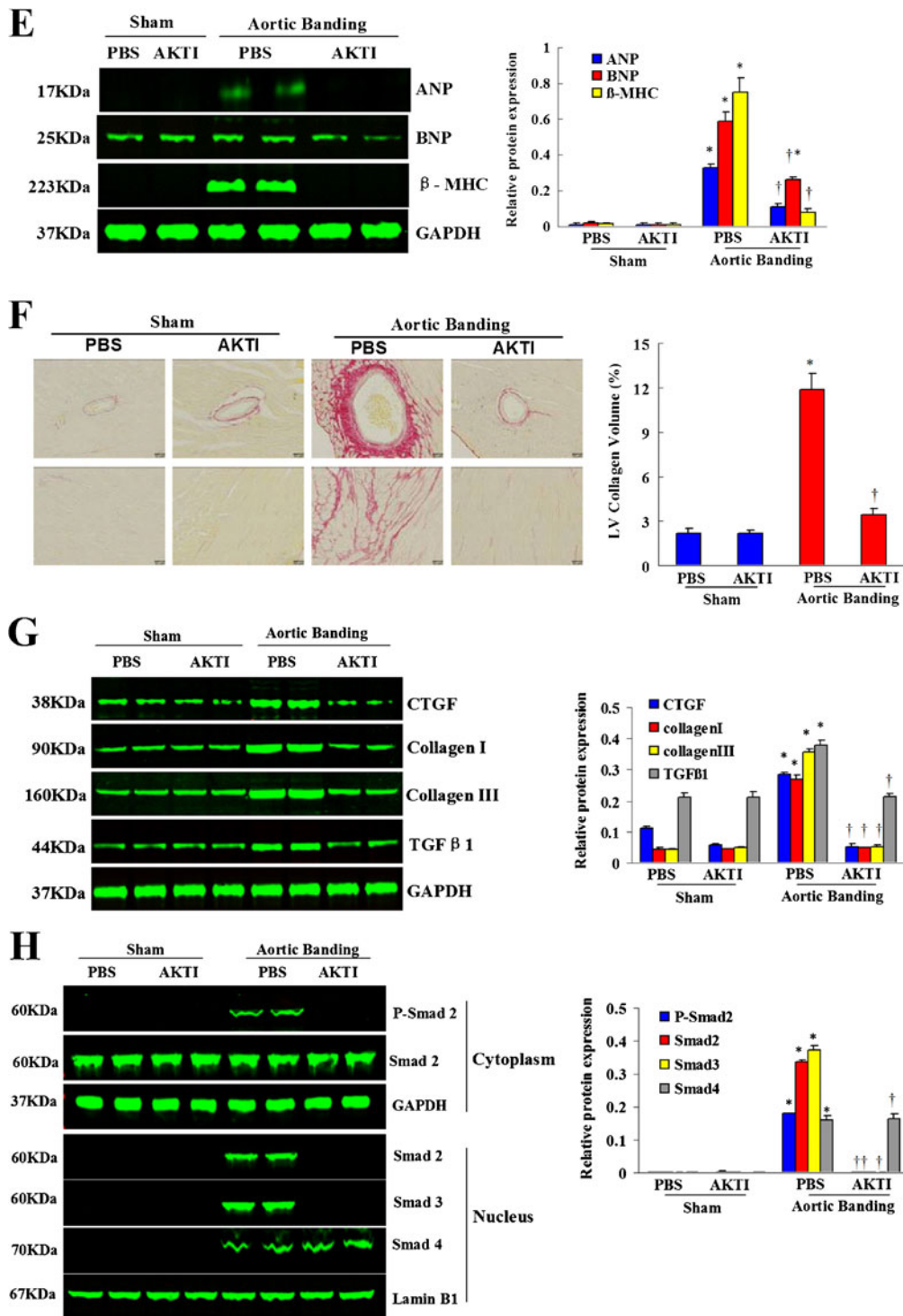
**Fig. 5** (continued)

activation results in "pathological" hypertrophy with a massive increase in heart size using cardiac-specific inducible AKT1 TG mice. Therefore, short-term AKT1 activation promotes physiological hypertrophy, whereas long-term AKT1 activation induces pathological hypertrophy in the heart [18–22]. In our current study, mice with mindin-deficient hearts showed markedly enhanced AKT signalling

mediated by a long-term 4-week aortic banding or Ang II infusion, which leads to aggravated pathological hypertrophy, interstitial fibrosis and cardiac dysfunction. Our findings are consistent with the above studies. Thus, mindin seems to be a more specific inhibitor of AKT signalling.

Fibrosis is another classical feature of pathological cardiac hypertrophy, which is characterised by the accumulation of
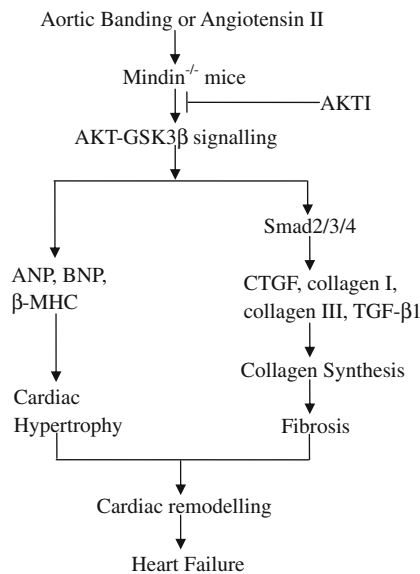
**Table 4** Echocardiographic and haemodynamics parameters in *Mindin*$^{-/-}$ mice after treatment with AKT inhibitor or saline

| Parameter | Saline–sham mice | AKTI–sham mice | Saline–AB mice | AKTI–AB mice |
|---|---|---|---|---|
| Number | 9 | 8 | 9 | 8 |
| BW (g) | 28.36±0.70 | 27.58±0.66 | 28.05±0.52 | 27.59±0.67 |
| HR (beats/min) | 505.82±9.69 | 494.86±9.13 | 503.49±12.03 | 500.38±6.99 |
| LVEDD (mm) | 3.71±0.01 | 3.63±0.07 | 5.28±0.09* | 3.90±0.01** |
| LVESD (mm) | 1.70±0.01 | 1.72±0.02 | 3.51±0.06* | 2.05±0.04** |
| IVSD (mm) | 0.66±0.02 | 0.63±0.01 | 1.05±0.01* | 0.69±0.01** |
| FS (%) | 54.31±0.26 | 56.62±2.00 | 33.41±1.12* | 47.46±1.19** |
| SBP (mmHg) | 112.5±4.6 | 115.1±3.3 | 154.5±6.1* | 155.1±5.8* |
| EF (%) | 56.7±3.5 | 56.9±4.4 | 29.6±6.5* | 44.6±5.1*, ** |
| LVEDP (mmHg) | 9.3±1.3 | 9.7±1.7 | 18.2±2.8* | 11.8±2.2** |
| LV $dP/dT_{max}$ (mmHg/s) | 8,768.4±567.1 | 8,992.6±511.4 | 7,153.8±448.7* | 8,459.1±489.4** |
| LV $dP/dT_{min}$ (mmHg/s) | −8,002.5±581.2 | −7,728.9±423.1 | −5,169.5±542.9* | −6,466.1±552.2** |

All values are mean±SEM

*$P<0.05$ versus saline sham; **$P<0.05$ versus saline–AB mice after 4 weeks AB

collagen. To date, approaches to restrain cardiac fibrosis have been limited. A better understanding of the mechanisms that stimulate collagen deposition in the heart may lead to novel strategies for suppressing cardiac fibrosis. This study, for the first time, reveals that mindin blocks



**Fig. 6** Proposed model of the effects of mindin deficiency on cardiac hypertrophy and fibrosis. Mindin deficiency enhances the activation of AKT/GSK3β signalling induced by aortic banding or Ang II infusion, which exacerbates cardiac remodelling. First, the activated AKT/GSK3β signalling pathway promotes hypertrophic marker expression and subsequently results in cardiac hypertrophy. Second, the AKT/GSK3β signalling pathway enhances Smad signalling, increases expression of fibrotic markers and leads to collagen synthesis and fibrosis. Mindin deficiency enhances these AKT-dependent signalling pathways and exacerbates cardiac hypertrophy and fibrosis, which promotes the progression of cardiac remodelling and heart failure. Pharmacological inhibition of AKT/GSK3β signalling rescues both cardiac hypertrophy and fibrosis in *Mindin*$^{-/-}$ mice in response to hypertrophic stimuli

cardiac fibrosis and attenuates the expression of several fibrotic mediators induced by chronic pressure overload or Ang II stimulation. The finding is consistent with the antifibrotic effects of integrin β1 and FAK [26–28]. In an attempt to elucidate the mechanisms underlying the inhibitory effect of mindin on fibrosis, we analysed key components of the TGF-β1-Smad signalling pathway, which plays an important role in the progression of fibrosis [28]. Our data demonstrate that mindin abrogates Smad2 phosphorylation and Smad2/3 translocation in hypertrophied hearts, thereby inhibiting fibrosis. We further examined the effects of AKT activation on fibrotic signalling. Using pharmacological inhibition of AKT/GSK3β signalling, we found that AKTI markedly reversed the exaggerated fibrosis found in *Mindin*$^{-/-}$ mice. Hye-Ryun et al. found that TGF-β1 activated phosphatidylinositol 3-kinase (PI3K) and AKT, and that AKT inhibition diminished TGF-β1-induced fibrosis [28]. As shown in Fig. 5g, AKTI markedly reduced the expression of TGF-β1 in *Mindin*$^{-/-}$ mice, which was followed by the elimination of Smad2 phosphorylation and Smad2/3 translocation in hypertrophied hearts. Therefore, mindin plays a central role in a PI3K/AKT-dependent pathway that contributes to TGF-β1/Smad-induced fibrosis and remodelling.

In conclusion, this study defines the role of mindin in cardiac hypertrophy and fibrosis. The molecular mechanisms responsible for the antihypertrophic and antifibrotic effects of mindin appear to be related to inhibition of the AKT/GSK3β signalling pathway. Our study provides insight into the pathogenesis of cardiac hypertrophy and may have significant implications for the development of novel strategies against cardiac remodelling and progression to HF by targeting mindin signalling.

# References

1. Berk BC, Fujiwara K, Lehoux S (2007) ECM remodeling in hypertensive heart disease. J Clin Invest 117:568–575

2. Chen H, Huang XN, Stewart AF, Sepulveda JL (2004) Gene expression changes associated with fibronectin-induced cardiac myocyte hypertrophy. Physiol Genomics 18:273–283

3. Brancaccio M, Fratta L, Notte A, Hirsch E, Poulet R, Guazzone S, De Acetis M, Vecchione C, Marino G, Altruda F et al (2003) a muscle-specific integrin beta1-interacting protein, is required to prevent cardiac failure in response to chronic pressure overload. Nat Med 9:68–75

4. Wang J, Hoshijima M, Lam J, Zhou Z, Jokiel A, Dalton ND, Hultenby K, Ruiz-Lozano P, Ross J Jr, Tryggvason K et al (2006) Cardiomyopathy associated with microcirculation dysfunction in laminin alpha4 chain-deficient mice. J Biol Chem 281:213–220

5. Feinstein Y, Klar A (2004) The neuronal class 2 TSR proteins F-spondin and *Mindin*: a small family with divergent biological activities. Int J Biochem Cell Biol 36:975–980

6. Jia W, Li H, He YW (2005) The extracellular matrix protein mindin serves as an integrin ligand and is critical for inflammatory cell recruitment. Blood 106:3854–3859

7. Li H, Oliver T, Jia W, He YW (2006) Efficient dendritic cell priming of T lymphocytes depends on the extracellular matrix protein mindin. EMBO J 25:4097–4107

8. He YW, Li H, Zhang J, Hsu CL, Lin E, Zhang N, Guo J, Forbush KA, Bevan MJ (2004) The extracellular matrix protein mindin is a pattern-recognition molecule for microbial pathogens. Nat Immunol 5:88–97

9. Yan L, Wei X, Tang QZ, Feng J, Zhang Y, Liu C, Bian ZY, Zhang LF, Chen M, Bai X et al (2011) Cardiac-specific mindin over-expression attenuates cardiac hypertrophy via blocking AKT/GSK3β and TGF-β1-Smad signalling. Cardiovasc Res 92:85–94

10. Bian ZY, Huang H, Jiang H, Shen DF, Yan L, Zhu LH, Wang L, Cao F, Liu C, Tang QZ et al (2010) LIM and cysteine-rich domains 1 regulates cardiac hypertrophy by targeting calcineurin/nuclear factor of activated T cells signaling. Hypertension 55:257–263

11. Li H, He C, Feng J, Zhang Y, Tang Q, Bian Z, Bai X, Zhou H, Jiang H, Heximer SP et al (2010) Regulator of G protein signaling 5 protects against cardiac hypertrophy and fibrosis during biomechanical stress of pressure overload. Proc Natl Acad Sci U S A 107:13818–13823

12. Li H, Tang QZ, Liu C, Moon M, Chen M, Yan L, Bian ZY et al (2010) Cellular FLICE-inhibitory protein protects against cardiac remodeling induced by angiotensin II in mice. Hypertension 56:1109–1117

13. Li HL, Zhuo ML, Wang D, Wang AB, Cai H, Sun LH, Yang Q, Huang Y, Wei YS, Liu PP et al (2007) Targeted cardiac over-expression of A20 improves left ventricular performance and reduces compensatory hypertrophy after myocardial infarction. Circulation 115:1885–1894

14. Li HL, Wang AB, Huang Y, Liu DP, Wei C, Williams GM, Zhang CN, Liu G, Liu YQ, Hao DL et al (2005) Isorhapontigenin, a new resveratrol analog, attenuates cardiac hypertrophy via blocking signaling transduction pathways. Free Radic Biol Med 38:243–257

15. Li HL, Huang Y, Zhang CN, Liu G, Wei YS, Wang AB, Liu YQ, Hui RT, Wei C, Williams GM et al (2006) Epigallocatechin-3 gallate inhibits cardiac hypertrophy through blocking reactive oxidative species-dependent and -independent signal pathways. Free Radic Biol Med 40:1756–1775

16. Cai J, Yi FF, Bian ZY, Shen DF, Yang L, Yan L, Tang QZ, Yang XC, Li H (2009) Crocetin protects against cardiac hypertrophy by blocking MEK-ERK1/2 signaling pathway. J Cell Mol Med 13:909–925

17. Tang Q, Cai J, Shen D, Bian Z, Yan L, Wang YX, Lan J, Zhuang GQ, Ma WZ, Wang W (2009) Lysosomal cysteine peptidase cathepsin L protects against cardiac hypertrophy through blocking AKT/GSK3beta signaling. J Mol Med 87:249–260

18. Heineke J, Molkentin JD (2006) Regulation of cardiac hypertrophy by intracellular signalling pathways. Nat Rev Mol Cell Biol 7:589–600

19. Shiojima I, Walsh K (2006) Regulation of cardiac growth and coronary angiogenesis by the Akt/PKB signaling pathway. Genes Dev 20:3347–3365

20. Chaanine AH, Hajjar RJ (2011) AKT signalling in the failing heart. Eur J Heart Fail 13:825–829

21. Terai Y, Abe M, Miyamoto K, Koike M, Yamasaki M, Ueda M, Ueki M, Sato Y (2001) Vascular smooth muscle cell growth-promoting factor/F-spondin inhibits angiogenesis via the blockade of integrin alphavbeta3 on vascular endothelial cells. J Cell Physiol 188:394–402

22. Matsui T et al (2002) Phenotypic spectrum caused by transgenic overexpression of activated Akt in the heart. J Biol Chem 277:22896–22901

23. Shioi T et al (2002) Akt/protein kinase B promotes organ growth in transgenic mice. Mol Cell Biol 22:2799–2809

24. Condorelli G et al (2002) Akt induces enhanced myocardial contractility and cell size in vivo in transgenic mice. Proc Natl Acad Sci USA 99:12333–12338

25. Taniyama Y, Ito M, Sato K, Kuester C, Veit K, Tremp G, Liao R, Colucci WS, Ivashchenko Y, Walsh K et al (2005) Akt3 over-expression in the heart results in progression from adaptive to maladaptive hypertrophy. J Mol Cell Cardiol 38:375–385

26. Shai SY, Harpf AE, Babbitt CJ, Jordan MC, Fishbein MC, Chen J, Omura M, Leil TA, Becker KD, Jiang M et al (2002) Cardiac myocyte-specific excision of the beta1 integrin gene results in myocardial fibrosis and cardiac failure. Circ Res 90:458–464

27. Peng X, Kraus MS, Wei H, Shen TL, Pariaut R, Alcaraz A, Ji G, Cheng L, Yang Q, Kotlikoff MI et al (2006) Inactivation of focal adhesion kinase in cardiomyocytes promotes eccentric cardiac hypertrophy and fibrosis in mice. J Clin Invest 116:217–227

28. Kang HR, Lee CG, Homer RJ, Elias JA (2007) Semaphorin 7A plays a critical role in TGF-beta1-induced pulmonary fibrosis. J Exp Med 204:1083–1093